

# Evidence for inelastic processes for $N_3^+$ and $N_4^+$ from ion energy distributions in He/ $N_2$ radio frequency glow discharges

Helen H. Hwang

*Department of Electrical and Computer Engineering, University of Illinois, 1406 West Green Street, Urbana, Illinois 61801*

James K. Olthoff, Richard J. Van Brunt, and Svetlana B. Radovanov

*National Institute of Standards and Technology, Electricity Division, Electronics and Electrical Engineering Laboratory, Gaithersburg, Maryland 20899*

Mark J. Kushner<sup>a)</sup>

*Department of Electrical and Computer Engineering, University of Illinois, 1406 West Green Street, Urbana, Illinois 61801*

(Received 17 May 1995; accepted for publication 19 September 1995)

The ion energy distributions (IEDs) striking surfaces in rf glow discharges are important in the context of plasma etching during the fabrication of microelectronics devices. In discharges sustained in molecular gases or multicomponent gas mixtures, the shape of the IED and the relative magnitudes of the ion fluxes are sensitive to ion–molecule collisions which occur in the presheath and sheath. Ions which collisionlessly traverse the sheaths or suffer only elastic collisions arrive at the substrate with a measurably different IED than do ions which undergo inelastic collisions. In this article we present measurements and results from parametric calculations of IEDs incident on the grounded electrode of a rf glow discharge sustained in a He/ $N_2$  gas mixture while using a Gaseous Electronics Conference Reference Cell (33.3 Pa, 13.56 MHz). We found that the shape of the IEDs for  $N_3^+$  and  $N_4^+$  provide evidence for inelastic ion–molecule reactions which have threshold energies of  $<10$  eV. © 1996 American Institute of Physics. [S0021-8979(96)07101-3]

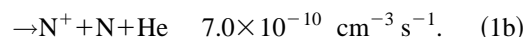
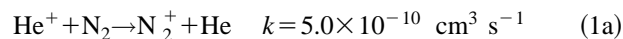
## I. INTRODUCTION

Low pressure rf discharges are commonly used for the etching of semiconductor materials for microelectronics devices in order to achieve anisotropic vertical features while eliminating undercutting of masks.<sup>1</sup> In these discharges, ions which are generated in the plasma are accelerated through the sheaths at the electrodes and so are vertically directed into the wafer. The arrival of this anisotropic ion flux on the bottom of trenches preferentially activates etching at those locations with respect to sidewalls, thereby producing the desired features. The importance of the distributions of ion energies and angles striking the wafer in obtaining straight walled features has long been recognized, and has motivated computational studies and experimental measurements of ion energy distributions (IEDs) in rf glow discharges.<sup>2–11</sup> Results of those studies have shown that both elastic and inelastic (charge exchange) collisions contribute to the broadening (in angular spread) and degradation (in energy) of the IED.

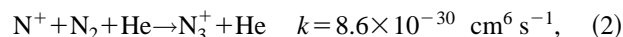
In rf discharges sustained in a single rare gas, the only important collisions for the dominant ions are elastic (momentum transfer which may include an energy loss for similar masses) and symmetric charge exchange. Symmetric charge exchange collisions in the sheaths are very efficient in degrading the IED. Due to the rapid rate of thermalization between collision partners having comparable masses, elastic collisions can contribute to both the broadening and degradation of the IED. The situation is more complex in molecular gases and in gas mixtures. In these discharges, collisions which change the identity of the ion can occur and ion–

molecule reactions having significant activation energy barriers may be important. These latter collisions are energetically forbidden in the bulk plasma where the ion energies are near thermal, but can occur in the high local electric fields of the sheaths where ions are accelerated to more than 10 eV. The threshold energy for these processes may result from the reaction being endothermic, or because there is an activation energy for either an exothermic or endothermic process. For simplicity in this article, we will refer to both classes of reactions as “barrier limited” processes.

In this article, we report on computed and experimentally measured IEDs in rf glow discharges sustained in He/ $N_2$  gas mixtures. This gas mixture was chosen for study because of its large variety of identity changing ion–molecule reactions (e.g.,  $He^+ + N_2 \rightarrow N_2^+ + He$ ), the possibility of barrier limited ion–molecule reactions (e.g.,  $N_2^+ + He \rightarrow N_2 + He^+$ ), and the absence of negative ions. In this gas mixture,  $He^+$  ions are initially produced by electron impact.  $N^+$  and  $N_2^+$  are dominantly produced by electron impact on  $N_2$  and charge exchange from  $He^+$  to  $N_2$  (Ref. 12).



(All rate coefficients are for an ion temperature of 300 K.) Higher order nitrogen ions,  $N_3^+$  and  $N_4^+$ , are then produced by associative ion molecule reactions with  $N_2$ ,<sup>12</sup>



<sup>a)</sup>Electronic mail: mjk@uiuc.edu

The trimer and tetrad ions have lower ionization potentials than any other neutral atom or molecule in the discharge, have no neutral counterparts, and have large masses. As a consequence, they cannot undergo exothermic or symmetric charge exchange reactions in the bulk plasma, and they lose little momentum during elastic collisions with lighter collision partners. In spite of these conditions, the shapes of the IEDs of  $N_3^+$  and  $N_4^+$  striking the electrodes in our experiments differ from that which one expects for purely elastic transport. In his review, Phelps<sup>13</sup> notes that dissociation of  $N_3^+$  and  $N_4^+$  in collisions with  $N_2$  are most likely important, but the lack of transport data prevents the drawing of any quantitative conclusions as to the thresholds and magnitudes of those cross sections. Our experimentally measured IEDs for  $N_3^+$  and  $N_4^+$  suggest the same. In the remainder of this article, we will discuss these observations and results of our calculations as evidence for the presence of reactions that destroy  $N_3^+$  and  $N_4^+$  by high energy collisions, and thus preferentially deplete the high energy portion of the energy distribution of these ions.

## II. EXPERIMENTAL APPARATUS

Ion energy distributions striking the grounded electrode were measured in a Gaseous Electronics Conference Reference Cell (GECRC).<sup>14</sup> The GECRC is a capacitively coupled rf discharge chamber equipped with two 10.2-cm-diam, parallel-plate, aluminum electrodes separated by 2.54 cm.<sup>15</sup> The upper electrode is grounded and the lower electrode is coupled to a 13.56 MHz rf power supply through a 0.1  $\mu$ F blocking capacitor. Gas is flowed into the plasma through a showerhead arrangement of small holes in the lower electrode. Mixtures of ultrahigh purity helium and nitrogen gases were used in this experiment and supplied through mass flow controllers.

The mass-analyzed IEDs were measured with an electrostatic energy analyzer (ESA) coupled to a quadrupole mass spectrometer (QMS) mounted on top of the GECRC to allow sampling of positive ions through a 0.1 mm orifice in the grounded electrode.<sup>16</sup> The IEDs were obtained by setting the quadrupole to a particular mass-to-charge ratio ( $m/z$ ), and then scanning the energy of the ions transmitted through the ESA. The energy resolution of the ESA is approximately 1.5 eV (full width at half-maximum) for the operating conditions used here. This method has been shown to be appropriate in rare gas plasmas.<sup>11,16</sup> Extension to discharge systems containing molecular gases is straightforward, primarily involving the investigation of a greater number of ions.

## III. DESCRIPTION OF THE MODEL

Theoretical IEDs were computed using a one-dimensional Monte Carlo–fluid hybrid (MCFH) model for rf discharges. The MCFH model has been previously described, and so will only be briefly discussed here.<sup>17–19</sup> The model combines a Monte Carlo simulation (MCS) for the nonequilibrium transport of electrons and ions with a fluid model for total charge densities and electric fields. The trajectories of electron and ion pseudoparticles are followed in the MCS module using the time and spatially varying electric fields

provided by the fluid module. All pertinent elastic and inelastic collisions are included in the MCS. Electron impact source functions and transport coefficients are obtained from the MCS and transferred to the fluid module. In the fluid module, the continuity equations for charged and neutral species and Poisson's equation for the electric field are solved. Although this simulation is one-dimensional, we specify a dc bias on one of the electrodes to approximate the operating conditions of an asymmetric discharge. Electric fields and species' densities are transferred back to the MCS, and the modules are iterated until convergence.

The results we report on here use a gas composition of He/ $N_2$ =50/50. The ions we considered are  $He^+$ ,  $N_2^+$ ,  $N^+$ ,  $N_3^+$ , and  $N_4^+$ . Electron impact processes and ion molecule reactions included in the model are discussed in Ref. 17. The endothermic cross section we used for reactions between  $N_2^+$  with He was reduced from that used in Ref. 19 based on comparisons of our simulations with the present experimental findings.<sup>20</sup> We additionally included the cross sections for ion–molecule reactions tabulated by Phelps for  $N_2$  gas mixtures.<sup>13</sup>

Calculating the IEDs with our model obviously requires the cross sections for the various collisions that ions undergo. In the absence of experimental or theoretical values, these cross sections must be estimated. The shape of the experimental IED can yield information on the existence and strength of inelastic barrier limited ion processes in the same fashion that the shape of electron energy distributions yield information on inelastic electron collisions. These observations can be used to both estimate barrier limited cross sections and, by comparing computed IEDs with the experiments, iteratively improve upon those estimates. To investigate the possibility of  $N_3^+$  and  $N_4^+$  barrier limited processes, we have simulated two scenarios. The first assumes only elastic collisions for ion transport of  $N_3^+$  and  $N_4^+$ . The second allows for barrier limited charge exchange reactions with  $N_2$ , using parametrized cross sections derived from comparisons to the experiments.

## IV. EXPERIMENTAL AND COMPUTED IEDS FOR He/ $N_2$ MIXTURES

The experimentally measured IEDs striking the grounded electrode for our conditions are shown in Fig. 1 for a 50/50 He/ $N_2$  plasma with an applied peak-to-peak rf voltage ( $V_{rf}$ ) of 200 V, a pressure of 33.3 Pa (250 mTorr), and a measured dc bias voltage of  $-43$  V. The  $He^+$  IED has two predominant structures, one occurring at low ion energies, and the other at 10–20 eV. The dominant low energy peak results from  $He^+$  ions which have suffered symmetric charge exchange or elastic collisions with He in the sheath. The high energy tail extending beyond 20 eV results from  $He^+$  which are produced in the sheath or presheath and proceed collisionlessly to the electrode. The shape of the IED may also suggest that the sheath has a large resistive component, thereby emphasizing the low energy (as opposed to the high energy) portion of the distribution.

The IED for  $N_2^+$  has the highest flux to the electrodes and a shape which is somewhat similar to that of  $He^+$ . The IED has a low energy peak and a tail which extends to 20 eV.

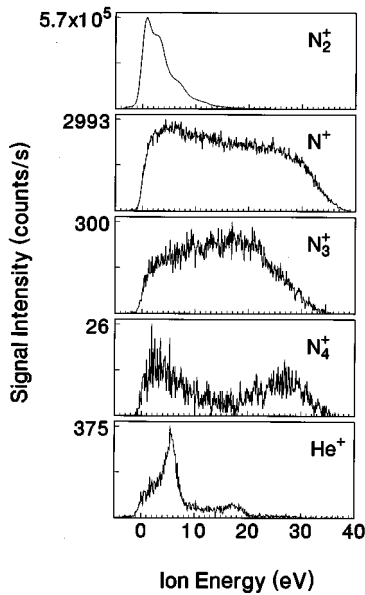


FIG. 1. Measured IEDs in a rf glow discharge sustained in a He/N<sub>2</sub> = 50/50, 33.3 Pa (250 mTorr) gas mixture,  $V_{rf}$  = 200 V (peak-to-peak) and  $V_{dc}$  = -43 V.

This shape, including the secondary maxima,<sup>16</sup> reflects the dominance of symmetric charge exchange collisions with N<sub>2</sub> in the sheaths. The IEDs for N<sup>+</sup>, N<sub>3</sub><sup>+</sup>, and N<sub>4</sub><sup>+</sup> extend to beyond 30 eV, suggesting that they are less energetically collisional than either He<sup>+</sup> or N<sub>2</sub><sup>+</sup>. Note that the magnitude of the fluxes for N<sub>3</sub><sup>+</sup> and N<sub>4</sub><sup>+</sup> are small compared to that for N<sub>2</sub><sup>+</sup> and N<sup>+</sup>, since the former ions are produced by three-body processes which have low rates at the pressures of interest.

The calculated IEDs for He<sup>+</sup>, N<sub>2</sub><sup>+</sup>, and N<sup>+</sup> striking the grounded electrode and powered electrode are shown in Fig. 2. We used the same conditions as in Fig. 1, except for a dc bias of -50 V. (The 7 V difference in dc biases does not appreciably alter the IEDs since the rf bias is much larger at 100 V amplitude.) The IEDs for N<sub>3</sub><sup>+</sup> and N<sub>4</sub><sup>+</sup> shown in Fig. 3 were obtained while having those ions undergo only elastic collisions. The calculated IEDs for He<sup>+</sup> and N<sub>2</sub><sup>+</sup> incident on the grounded electrode generally agree with those measured experimentally, as do the relative magnitudes of the fluxes. Both distributions are dominated by a low energy maximum resulting from symmetric charge collisions in the sheath. The IEDs have a tail extending to higher energies, a consequence of ions which collisionlessly traverse the sheath.

The experimental and calculated IEDs for N<sup>+</sup> extend to 30 eV, indicating that N<sup>+</sup> does not undergo significant symmetric charge exchange or energy loss collisions. The shape is not consistent, however, with purely elastic transport either. N<sup>+</sup> will undergo barrier limited collisions with N<sub>2</sub> producing N<sub>2</sub><sup>+</sup>. This process has a threshold energy of ≈ 1.7 eV. Its cross section has a local maximum at 30 eV of ≈ 5 × 10<sup>-16</sup> cm<sup>2</sup>.<sup>13</sup> The mean free path for the loss of N<sup>+</sup> at energies greater than 20 eV by this process is ≈ 0.5 cm, which is commensurate with the sheath width. The IED for N<sup>+</sup> is therefore depleted at these energies relative to the IED for purely elastic transport. N<sup>+</sup> can also be produced in the

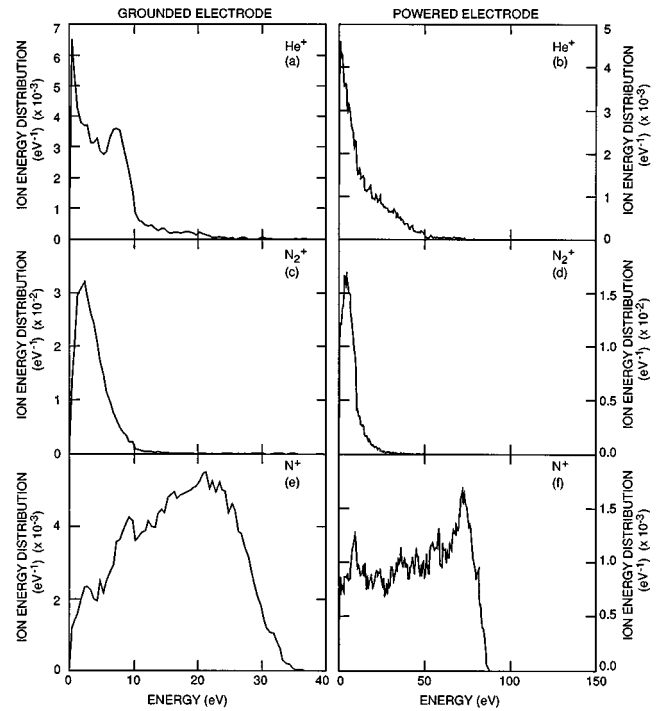


FIG. 2. Calculated IEDs for the conditions of Fig. 1, except  $V_{dc}$  = -50 V. IEDs in the left-hand column are for ions striking the grounded electrode. IEDs in the right-hand column are for ions striking the powered electrode. (a) and (b) He<sup>+</sup>, (c) and (d) N<sub>2</sub><sup>+</sup>, (e) and (f) N<sup>+</sup>. The calculated IEDs for He<sup>+</sup> and N<sub>2</sub><sup>+</sup> are dominated by low energy peaks resulting from symmetric charge exchange.

sheath by barrier limited reactions of N<sub>2</sub><sup>+</sup> with N<sub>2</sub> with a threshold energy of 15 eV.<sup>13</sup> This source of N<sup>+</sup> will occur deep into the sheath where N<sub>2</sub><sup>+</sup> ions have gained at least this energy. The N<sup>+</sup> ions so produced will preferentially arrive at the electrode with low energies.

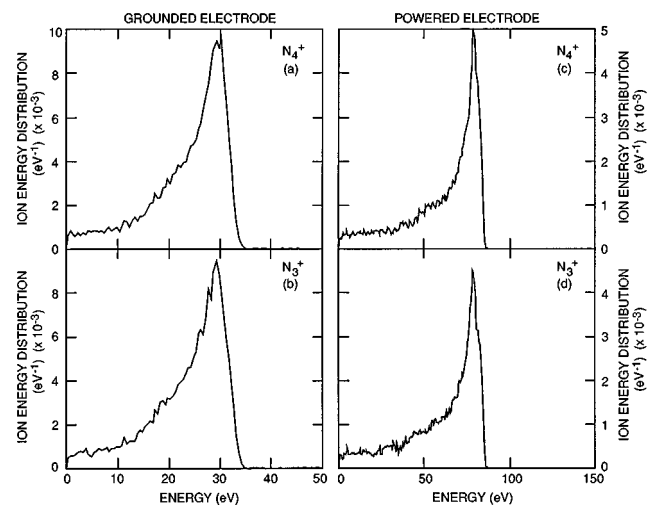
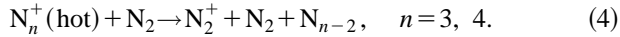


FIG. 3. Calculated IEDs for N<sub>3</sub><sup>+</sup> and N<sub>4</sub><sup>+</sup> striking the grounded (left-hand column) and powered (right-hand column) electrodes for the conditions of Fig. 1. (a) and (c) N<sub>4</sub><sup>+</sup>, (b) and (d) N<sub>3</sub><sup>+</sup>. For these results, N<sub>3</sub><sup>+</sup> and N<sub>4</sub><sup>+</sup> undergo only elastic collisions. The disparate shape of the IEDs compared to the measurements suggest that N<sub>3</sub><sup>+</sup> and N<sub>4</sub><sup>+</sup> additionally suffer barrier limited inelastic collisions.

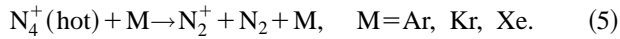
The IEDs incident on the powered electrode retain the same general structure, though extended to higher energy due to the larger sheath potential. The maximum energy with which ions can strike the powered electrode is approximately the sum of the rf amplitude, magnitude of the dc bias, and floating potential,  $\approx 160$  eV in this case. Due to the ion transit time across the sheath for heavy ions exceeding many rf cycles, the practical maximum energy is approximately half the maximum, or 75–80 eV.

The IEDs for  $N_3^+$  and  $N_4^+$  shown in Fig. 3 differ noticeably from the experiments. Since  $N_3^+$  and  $N_4^+$  are both heavy compared to their neutral elastic collision partners, they lose little momentum during those collisions. As a result, the IEDs of these ions have their peaks at nearly the maximum allowed energies (accounting for long transit times through the sheath). The disparity between the model and experiments discounts the assumption that these ions have only elastic collisions in the sheaths. Since the ionization energies of  $N_3^+$  and  $N_4^+$  are smaller than He, N, or  $N_2$ , exothermic inelastic charge exchange collisions cannot occur.<sup>21</sup> Therefore, the dissimilarity in the calculated and observed IEDs is likely due to the absence of barrier limited ion molecule collisions in the calculation.

To test this hypothesis, we proposed barrier limited ion-molecule reactions for  $N_3^+$  and  $N_4^+$  of the form of



In principal, this reaction could be a dissociative charge exchange collision or a “direct” bond breaking collision. The latter class of interaction has been experimentally observed by Shultz and Armentrout<sup>21</sup> for collisions of  $N_4^+$  with rare gases,



Bond breaking can result directly from excitation of  $N_4^+$  to a dissociative state or through formation of a dissociative intermediate (e.g.,  $N_4^+M \rightarrow N_2^+M + N_2 \rightarrow N_2^+ + M + N_2$ ). Lacking experimental data for the cross sections of the proposed reaction, we parametrized the cross sections. For purposes of demonstration, we assumed the dissociative reaction proceeded through the charge exchange channel and initially set the threshold energies for these processes equal to the differences in the ionization potentials of the collision partners,  $\epsilon_0$ . This yields threshold energies for  $N_3^+$  and  $N_4^+$  of  $\epsilon_0 = 1.07$  and 4.08 eV, respectively, which are comparable to those for the direct process of  $N_4^+$  with some of the rare gases.<sup>21</sup> We then implemented the parametric form for barrier limited ion-molecule cross sections suggested by Fisher *et al.*<sup>20</sup> For our conditions, this resulted in a cross section which decreased for energies above 15–20 eV and did not sufficiently deplete the calculated IED of high energy ions as is observed experimentally. We next used parametrically defined step function cross sections beginning at a threshold energy  $\Delta\epsilon$  and having a magnitude  $\sigma_m$  with the goal of depleting the higher energy ions in the IED. We derived the magnitudes of the cross section and the threshold energies by comparing the results of our parametrizations with the experiments.

Results from our parametrizations for the IEDs of  $N_3^+$  and  $N_4^+$  striking the grounded electrode are shown in Fig. 4.

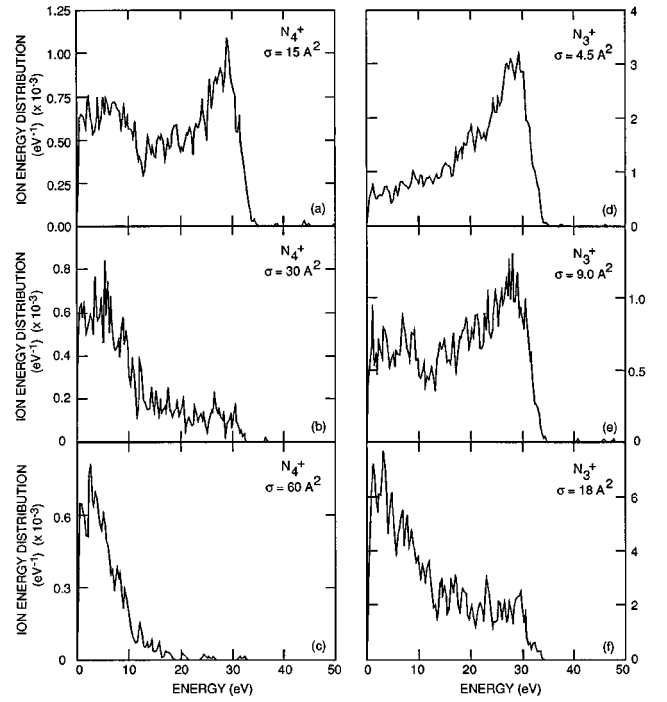


FIG. 4. IEDs for  $N_4^+$  [(a)–(c)] and  $N_3^+$  [(d)–(f)] striking the grounded electrode obtained while varying  $\sigma_m$  in step function cross sections.  $\sigma_m$  for  $N_4^+$  was varied from 15 to  $60 \times 10^{-16}$  cm<sup>2</sup>.  $\sigma_m$  for  $N_3^+$  were varied from 4.5 to  $18 \times 10^{-16}$  cm<sup>2</sup>. The threshold energies are fixed at their thermodynamic values ( $\Delta\epsilon = 1.07$  and 4.08 eV for  $N_3^+$  and  $N_4^+$ , respectively). Increasing  $\sigma_m$  depletes the high energy portion of the IED.

The threshold energies are fixed at their thermodynamic values  $\epsilon_0$  ( $\Delta\epsilon = 1.07$  and 4.08 eV for  $N_3^+$  and  $N_4^+$ , respectively). The cross section was varied between 4.5 and  $18 \times 10^{-16}$  cm<sup>2</sup> for  $N_3^+$ ; and between 15 and  $60 \times 10^{-16}$  cm<sup>2</sup> for  $N_4^+$ . (Note that the IEDs are numerically noisier than those obtained assuming elastic collisions, since the barrier limited collisions physically remove  $N_3^+$  and  $N_4^+$  ions from the simulation, thus leading to smaller numbers of pseudoparticles collected on the electrodes.) Focusing first on the IEDs for  $N_4^+$ , we see that in all cases the inelastic charge exchange process depletes the IED of high energy ions relative to the distribution obtained using only elastic collisions (see Fig. 3). The experimentally observed peak in the IED at  $\approx 28$  eV is captured in the calculations using the smaller cross sections. The depletion of the IED at high energies is too severe when using the larger cross section, and the high energy peak is lost. The flux of  $N_4^+$  to the substrate monotonically decreases as  $\sigma_m$  increases as more of those ions are lost by charge exchange collisions. Comparing these IEDs to the experiment indicates that the inelastic cross section is likely to be in the range  $15\text{--}30 \times 10^{-16}$  cm<sup>2</sup>.

The IEDs for  $N_3^+$  have a similar appearance to those for  $N_4^+$ . The IEDs have a peak at high energy with the smaller cross section, somewhat resembling the case with only elastic collisions. Increasing the cross section depletes the IED at high energies relative to the low energies. There is a rapid transition between an IED having a high energy peak and one dominated by the low energy peak between 9 and  $18 \times 10^{-16}$  cm<sup>2</sup>. The experimental IED for  $N_3^+$  is broadly peaked at  $\approx 20$  eV. The inelastic cross section which repro-

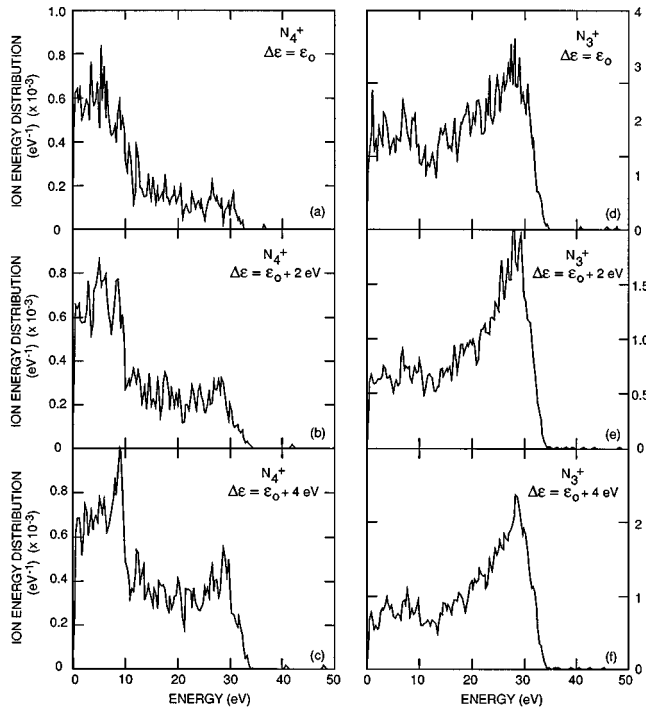


FIG. 5. IEDs for  $N_4^+$  [(a)–(c)] and  $N_3^+$  [(d)–(f)] striking the grounded electrode obtained while varying  $\Delta\epsilon$  using step function cross sections.  $\Delta\epsilon$  was varied from  $\epsilon_0$  to  $\epsilon_0 + 4$  eV. ( $\epsilon_0 = 1.07$  and  $4.08$  eV for  $N_3^+$  and  $N_4^+$ , respectively.)  $\sigma_m$  was fixed at  $9$  and  $30 \times 10^{-16}$  cm $^2$  for  $N_3^+$  and  $N_4^+$ . The high energy portion of the IED increases with increasing  $\Delta\epsilon$ , though the effect is not large.

duces this shape likely has a cross section in the range of  $9$ – $18 \times 10^{-16}$  cm $^2$ , however the IED appears to be poorly represented by a step function for the inelastic process.

The IEDs for  $N_3^+$  and  $N_4^+$  for varying threshold energies are shown in Fig. 5. In each case, the threshold energy was incremented by  $2$  and  $4$  eV from their thermodynamic values,  $\epsilon_0$ . The cross sections have  $\sigma_m = 9$  and  $30 \times 10^{-16}$  cm $^2$  for  $N_3^+$  and  $N_4^+$ . The IEDs for  $N_4^+$  at high energy increase with increasing threshold energy relative to the low energy portion of the IED. With increasing threshold energy, more ions survive the relatively thick presheath region where their energies are  $< 10$  eV, and so are available to be accelerated to higher energies in the sheath proper. The effect, however, is not large. Significant changes in the IED would require increases in threshold energy to  $> 10$ – $15$  eV. The trend is similar for the IEDs of  $N_3^+$ . With increasing threshold energy, the IED at high energy increases relative to that for low energy.

Calculated IEDs appear in Fig. 6 for  $N_3^+$  and  $N_4^+$  with cross-section parameters derived by comparing our previous results with the experimental IEDs. These parameters are  $\Delta\epsilon = \epsilon_0$  ( $1.07$  eV) and  $\sigma_m = 1.13 \times 10^{-15}$  cm $^2$  for  $N_3^+$ ; and  $\Delta\epsilon = 2\epsilon_0$  ( $8.08$  eV) and  $\sigma_m = 2.25 \times 10^{-15}$  cm $^2$  for  $N_4^+$ . The experimental IEDs are also reproduced in Fig. 6. These IEDs should be compared to those in Fig. 3 obtained using only elastic collisions. The calculated IED for  $N_4^+$  agrees well with the experiment. It has a double peak shape with a maximum value at a few eV and the secondary peak at  $\approx 28$  eV, as in the experiments. The derived value for  $\sigma_m$  is large enough

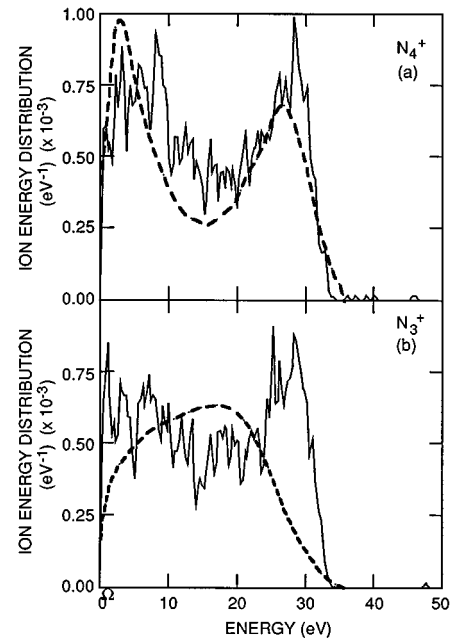


FIG. 6. IEDs for  $N_3^+$  and  $N_4^+$  striking the grounded electrode using derived step function cross sections (solid lines) with comparison to experimental IEDs (dashed lines). (a)  $N_4^+$ ,  $\sigma_m = 2.25 \times 10^{-15}$  cm $^2$ ,  $\Delta\epsilon = 2\epsilon_0$  ( $8.08$  eV); (b)  $N_3^+$ ,  $\sigma_m = 1.13 \times 10^{-15}$  cm $^2$ ,  $\Delta\epsilon = \epsilon_0$  ( $1.07$  eV). The calculated IED for  $N_4^+$  using a step function cross section captures the shape of the experimental IED, however the  $N_3^+$  IED is not well represented.

to deplete the IED above the inelastic threshold, and has a high enough threshold energy to allow some ions to collisionlessly cross the sheath and populate the tail of the distribution. The IED for  $N_3^+$  has the appropriately broadened shape with a width of  $30$  eV. However, the IED is more heavily populated in the tail than in the experiment. Our experience is that the experimental IED for  $N_3^+$  cannot be well fit by our calculations using a step cross section. This result suggests that the cross section likely increases with increasing energy through tens of eV.

## V. CONCLUDING REMARKS

Measurements and calculations of ion energy distributions for a He/ $N_2$  rf glow discharge have been presented. In spite of the fact that the ionization potentials of  $N_3^+$  and  $N_4^+$  are the lowest in the system, the measured shapes of the IEDs for  $N_3^+$  and  $N_4^+$  are inconsistent with these ions traversing the sheaths suffering only elastic collisions. Calculated IEDs which agree reasonably well with the measurements were obtained by proposing inelastic ion–molecule reactions for  $N_3^+$  and  $N_4^+$  with  $N_2$  having threshold energies of  $< 10$  eV. The model cross sections were step functions of magnitude  $1.1$  and  $2.2 \times 10^{-15}$  cm $^2$  for  $N_3^+$  and  $N_4^+$ . The threshold energies were  $\Delta\epsilon = \epsilon_0$  ( $1.07$  eV) and  $2\epsilon_0$  ( $8.08$  eV), respectively. The shape of the measured IEDs, however, suggest that there may be structure to the cross sections for energies of  $10$ – $30$  eV, particularly for  $N_3^+$ . The proposed inelastic processes support the proposition of Phelps,<sup>13</sup> who cited evidence for the existence of inelastic collisions of  $N_3^+$  and  $N_4^+$  with  $N_2$ .

This evidence comes, in part, from drift tube experiments. The results of these experiments implied that the rate coefficient for dissociation of  $N_4^+$  steeply rises from  $10^{-13}$  to  $10^{-11}$   $\text{cm}^3 \text{s}^{-1}$  between reduced electric fields ( $E/N$ ) of 100 and 200 Td ( $1 \text{ Td} = 1 \times 10^{-17} \text{ V cm}^2$ ). The effective temperature of  $N_4^+$  at 200 Td, however, is only  $\approx 0.25 \text{ eV}$ .<sup>22</sup> The large rate coefficient for dissociation derived from the drift tube experiments cannot then be explained by the inelastic process used here since the implied cross section would be too large. At the same time, if the rate coefficient for dissociation has a value greatly exceeding  $10^{-11} \text{ cm}^3 \text{s}^{-1}$  at energies of many tenths of an eV, the  $N_4^+$  produced in the bulk plasma would be nearly depleted in the presheath. The experimentally observed IED for  $N_4^+$  would then have to result dominantly from formation of  $N_4^+$  in the sheath, which is not likely.

## ACKNOWLEDGMENTS

H.H.H. and M.J.K. were supported by the University of Wisconsin Engineering Research Center for Plasma Aided Manufacturing, the National Science Foundation (ECS94-04133, CTS94-12565), and the Semiconductor Research Corporation.

<sup>1</sup> *Plasma Etching: An Introduction*, edited by D. M. Manos and D. L. Flamm (Academic, Boston, 1989).

<sup>2</sup> A. Manenschijn and W. J. Goedheer, *J. Appl. Phys.* **69**, 2923 (1991).

<sup>3</sup> M. J. Kushner, *J. Appl. Phys.* **58**, 4024 (1985).

<sup>4</sup> B. E. Thompson, H. H. Sawin, and D. A. Fisher, *J. Appl. Phys.* **63**, 2241 (1988).

<sup>5</sup> J. Liu, G. L. Huppert, and H. H. Sawin, *J. Appl. Phys.* **68**, 3916 (1990).

<sup>6</sup> S. G. Ingram and N. St. J. Braithwaite, *J. Phys. D* **21**, 1496 (1988).

<sup>7</sup> A. D. Kuypers and H. J. Hopman, *J. Appl. Phys.* **67**, 1229 (1990).

<sup>8</sup> A. Manenschijn, G. C. A. M. Janssen, E. van der Drift, and S. Radelaar, *J. Appl. Phys.* **69**, 1253 (1991).

<sup>9</sup> D. Field, D. F. Klemperer, P. W. May, and Y. P. Song, *J. Appl. Phys.* **70**, 82 (1991).

<sup>10</sup> H. Toyoda, H. Kojima, and H. Sugai, *Appl. Phys. Lett.* **54**, 1507 (1989).

<sup>11</sup> J. K. Olthoff, R. J. Van Brunt, S. B. Radovanov, and J. A. Rees, *Proc. IEE Sci. Meas. Technol.* **141**, 105 (1994).

<sup>12</sup> D. L. Albritton, *At. Data. Nucl. Data Tables* **22**, 2 (1978).

<sup>13</sup> A. V. Phelps, *J. Phys. Chem. Ref. Data* **20**, 557 (1991).

<sup>14</sup> P. J. Hargis *et al.*, *Rev. Sci. Instrum.* **65**, 140 (1994).

<sup>15</sup> For the IEDs measured here, the grounded aluminum electrode was replaced with an identical stainless steel electrode to reduce surface charging and improve ion sampling through the orifice. Details are discussed in J. K. Olthoff, R. J. Van Brunt, and S. B. Radovanov, *Appl. Phys. Lett.* **67**, 473 (1995).

<sup>16</sup> J. K. Olthoff, R. J. Van Brunt, S. B. Radovanov, J. A. Rees, and R. Surowiec, *J. Appl. Phys.* **75**, 115 (1994).

<sup>17</sup> T. J. Sommerer and M. J. Kushner, *J. Appl. Phys.* **71**, 1654 (1992).

<sup>18</sup> T. J. Sommerer and M. J. Kushner, *J. Vac. Sci. Technol. B* **10**, 2179 (1992).

<sup>19</sup> H. H. Hwang and M. J. Kushner, *Plasma Sources Sci. Technol.* **3**, 190 (1994).

<sup>20</sup> E. R. Fisher, M. E. Weber, and P. B. Armentrout, *J. Chem. Phys.* **92**, 2296 (1990). The endothermic cross section for  $N_2^+$  with He has the proposed form with a maximum value of  $6 \times 10^{-16} \text{ cm}^2$ .

<sup>21</sup> R. H. Schultz and P. B. Armentrout, *Int. J. Mass Spectrosc. Ion Proc.* **107**, 29 (1991).

<sup>22</sup> H. W. Ellis, E. W. McDaniel, D. L. Albritton, L. A. Viehland, S. L. Lin, and E. A. Mason, *At. Data Nucl. Data Tables* **22**, 179 (1978).